

## CHAPTER 6

### Neutron induced reaction cross-section measurements for Zr isotopes

<b>6.1 Introduction</b>	<b>127</b>
<b>6.2 Experimental Method</b>	<b>129</b>
<b>6.2.1 Thermal neutron activation cross-section measurements of</b>	
$^{94}\text{Zr}(n,\gamma)^{95}\text{Zr}$ and $^{96}\text{Zr}(n,\gamma)^{97}\text{Zr}$ at APSARA reactor, B.A.R.C	129
<b>6.2.2 Measurement of <math>^{94}\text{Zr}(n,\gamma)^{95}\text{Zr}</math> reaction cross-section at <math>E_n=2.45</math> MeV,</b>	
Purnima Neutron Generator, B.A.R.C	131
<b>6.2.3 Measurement of <math>^{90}\text{Zr}(n,p)^{90}\text{Y}^m</math> reaction cross-section at average</b>	
$E_n = 9.85 \pm 0.38$ MeV, T.I.F.R-B.A.R.C Pelletron Facility	133
<b>6.3 Calculations</b>	<b>135</b>
<b>6.3.1 Calculations of neutron flux</b>	<b>135</b>
<b>6.3.2 Calculations of Neutron cross-section</b>	<b>137</b>
<b>6.4 Result and Discussions</b>	<b>139</b>
<b>6.5 Summary and Conclusions</b>	<b>142</b>
<b>References</b>	<b>143</b>

#### **Published in:**

1. P. M. Prajapati et al., *Measurement of neutron-induced reaction cross-sections in zirconium isotopes at thermal, 2.45 MeV and 9.85 MeV energies*, Nucl. Sci. Eng. **171**, 78 (2012)

## 6.1 Introduction

High quality and accurate nuclear data are essential for the design and analysis nuclear systems, such as reactor cores layout, fuel elements and stored mixtures of nuclear waste with other materials, as well as burned fuel elements. The measurement of neutron activation cross-sections and the improved nuclear database of these cross-sections play a vital role for the safe operation of various nuclear systems such as Gen-IV nuclear reactors, fusion reactors and the accelerator driven subcritical systems (ADS) [1, 2]. The neutron-induced activation cross-sections have direct applications in estimating radiation levels and decay heat of materials that have been exposed to radiation fields with strong neutron component [3]. The range of applications of neutron cross-section also covers environmental and space dosimetry, material analysis and isotope production [4, 5]. Besides these practical applications, a study of neutron-induced reactions  $(n, \gamma)$ ,  $(n, p)$ ,  $(n, \alpha)$ ,  $(n, 2n)$  etc. on various nuclei provides an experimental database for testing validity of theoretical nuclear physics models. Furthermore, the study of charged particle (proton and helium) emission cross-section is important as basic study. The contributions of the direct, pre-equilibrium and the statistical compound nucleus processes, in the emission of charged particles can be estimated for a given  $(n, z)$  reaction [6]. Neutron cross-section data are available from compilations of experimental data (EXFOR) or through evaluated and comprehensive evaluated nuclear data libraries (ENDF/B, JENDL and JEFF etc). It should be noted that the necessary update of these evaluated cross section libraries depends on the availability of accurate measurements obtainable with advanced neutron sources.

Neutron induced reaction cross-sections for structural materials (Zr, Ni, Fe, Al etc) are basic data for evaluation of the processes in materials under irradiation in nuclear reactors. Neutron-induced reactions on zirconium are of a particular importance in a wide range of applications. Zirconium is an important and major component of the structural materials used in traditional and advanced nuclear reactors, owing to its very low absorption cross-sections for thermal neutrons and resistance to corrosion. About ninety percent of zirconium produced is frequently used as cladding of fuel rods, calandria vessel and pipe lines of secondary coolant circuit in nuclear reactors in the form of Zircaloy. In addition to its use in current nuclear reactors, Zr is present in most of the innovative concepts [7, 8]. This implies cross-section data

needs in a broad energy range. However, its cross-sections database especially for neutron threshold reactions is rather sparse [9, 10].

A number of data were reported on neutron-induced reaction cross-sections for zirconium isotopes, and many of these were measured with the activation technique followed by off-line  $\gamma$ -ray spectrometric technique. Different neutron-emission reactions and incident charged particle energies are conventionally used for the production of quassi-monoenergetic neutrons in the energy range up to 20 MeV and this is reflected in the available experimental data base. The International Atomic Energy Agency-Exchange Format (IAEA-EXFOR) database [11] shows significant discrepancy and gaps in the measured experimental data for many neutron threshold reactions. It also indicates that there has been no neutron capture ( $n,\gamma$ ) reaction cross-section data available beyond the neutron energy of 2 MeV for many zirconium isotopes. Further, literature survey [12-19] shows that most of the thermal neutron activation cross-section measurements for zirconium isotopes were made in reactors with neutron spectra and thus were not precise for thermal neutrons.

The objective of the present work is to measure, the  $^{94}\text{Zr}(n,\gamma)^{95}\text{Zr}$  and  $^{90}\text{Zr}(n,p)^{90}\text{Y}^m$  reaction cross-sections at  $E_n = 2.45$  MeV and at average  $E_n = 9.85 \pm 0.38$  MeV respectively using neutron activation method and off-line  $\gamma$ -ray spectrometric technique. For the measurement of  $^{94}\text{Zr}(n,\gamma)^{95}\text{Zr}$  reaction cross-section at  $E_n = 2.45$ , Purnima Neutron Generator (PNG) facility at B.A.R.C, Mumbai has been utilized. PNG produces monoenergetic neutrons of energy 2.45 MeV based on the  $\text{D}(\text{D}, \text{n})^3\text{He}$  fusion reaction. The  $^{90}\text{Zr}(n,p)^{90}\text{Y}^m$  reaction cross-section at average  $E_n = 9.85 \pm 0.38$  MeV has been measured using BARC-TIFR Pelletron facility, Mumbai. The average neutrons of energy  $9.85 \pm 0.38$  MeV have been produced using  $^7\text{Li}(p,n)^7\text{Be}^*$  reaction at the six meter height main line above the analyzing magnet to utilize the maximum proton current from the accelerator. The “thermal neutron” activation cross-sections of  $^{94}\text{Zr}(n,\gamma)^{95}\text{Zr}$  and  $^{96}\text{Zr}(n,\gamma)^{97}\text{Zr}$  reactions were measured in the thermal column of swimming pool type APSARA reactor, B. A. R. C, Mumbai, India. The present measurement at thermal neutron energy ( $E_n = 0.0253$  eV) is compared with experimental data from IAEA-EXFOR and is used to validate the methodology applied here. The experimentally measured reaction cross-sections were compared

with evaluated nuclear data libraries of ENDF-VII/B [20], JENDL 4.0 [21] and TENDL 2010 [22].

## 6.2 Experimental Method

The measurement of neutron induced reaction cross-sections for zirconium isotopes were carried out using three separate irradiations at APSARA reactor, Purnima Neutron generator and BARC-TIFR Pelletron facility, Mumbai, India. Details of experimental procedure applied to measure the neutron cross-sections for three different irradiations are given below.

### 6.2.1 Thermal neutron activation cross-section measurements of $^{94}\text{Zr}(n,\gamma)^{95}\text{Zr}$ and $^{96}\text{Zr}(n,\gamma)^{97}\text{Zr}$ at APSARA reactor, B.A.R.C, Mumbai

A known amount (0.3268 gm) of natural Zr metal foil (17.38%  $^{94}\text{Zr}$ , 2.8%  $^{96}\text{Zr}$ ) of thickness about 1 mm and Au metal foil (0.0215 gm) for neutron flux monitor were wrapped separately with 0.025 mm thick super pure aluminum foil and doubly sealed with alkathene bags. These samples were kept inside an irradiation capsule made of polypropylene. The capsule containing samples were doubly resealed with alkathene bags and were taken for irradiation. These samples were irradiated in the thermal column of swimming pool type APSARA reactor for the period of 6 hours and 30 minutes. After sufficient cooling, the irradiated samples of Zr and Au along with Al wrapper were mounted on two different perspex plates and taken for  $\gamma$ -ray spectrometry. Radioactivity in the irradiated Zr and Au samples were measured using energy and efficiency calibrated 80 cm<sup>3</sup> high-purity germanium (HPGe) detector coupled to a PC-based 4K multi-channel analyzer in live time mode. The efficiency of the detector was 20 % with energy resolution of 2.0 keV FWHM at 1332.0 keV peak of  $^{60}\text{Co}$ . The standard  $^{152}\text{Eu}$  source having  $\gamma$ -rays in the energy range of 121.8-1408 keV was used for energy and efficiency calibration. The dead time of the detector system during counting was always kept less than 10 % by placing the sample at a suitable distance to avoid pile up effects. A typical  $\gamma$ -ray spectrum of  $\text{Zr}(n,\gamma)$  reaction from thermal neutron irradiation is shown in Fig. 6.1. The  $\gamma$ -ray spectrum was analyzed with PHAST peak fitting program [23], which can search for up to 500 peaks and fit model peak shape. Measured disintegration rates, based on the  $\gamma$ -ray energies of 724.9 keV and 756.72 keV for  $^{95}\text{Zr}$  and 743.36 keV for  $^{97}\text{Zr}$  confirmed that no interfering activities were present. The radioactive decay of the samples was followed to confirm the identity of nuclide being studied.

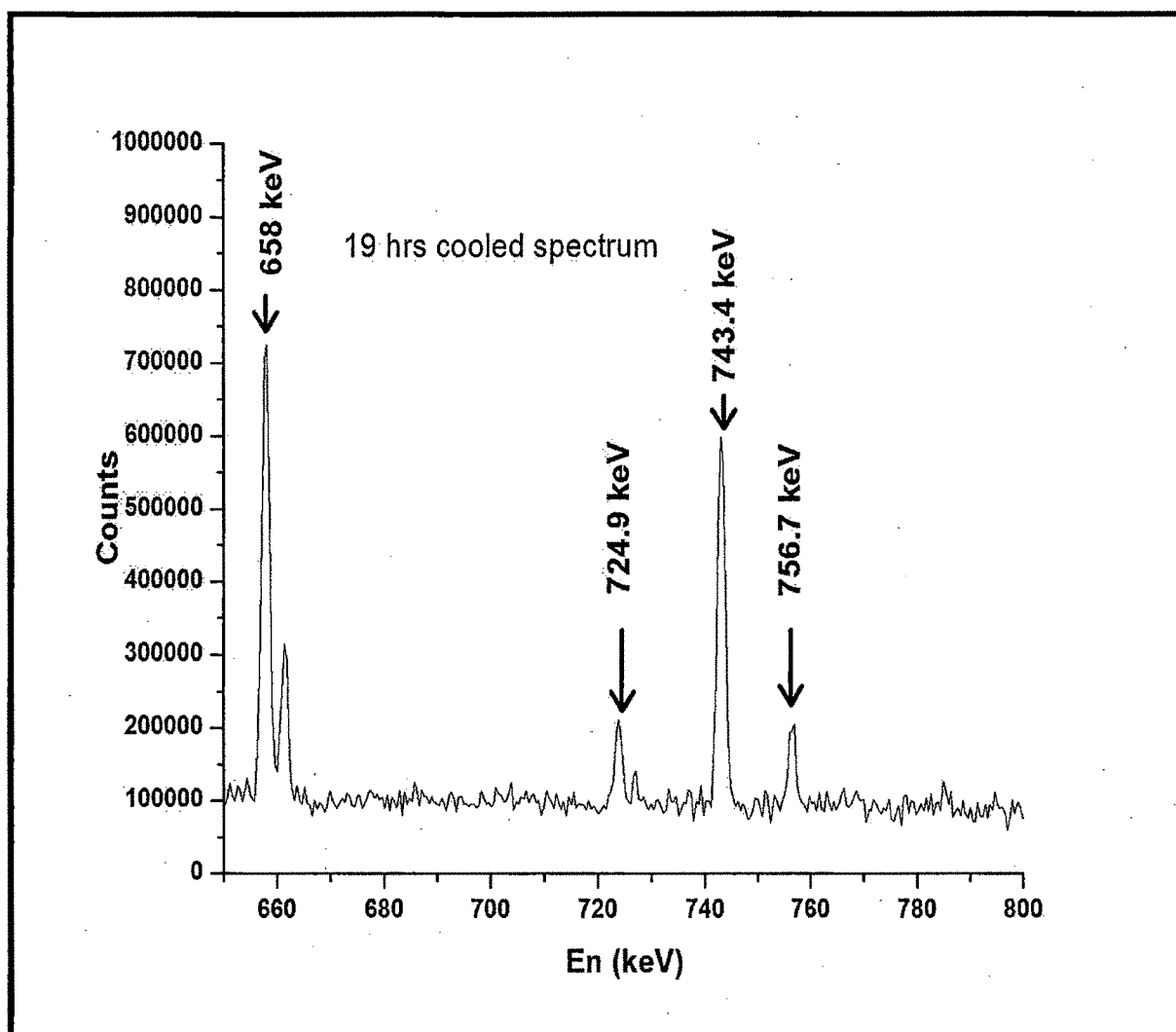


**Fig. 6.1** Typical  $\gamma$ -ray spectrum of irradiated natural Zr metal at thermal neutron energy in APSARA reactor showing the  $\gamma$ -ray energy of  $^{95}\text{Zr}$  and  $^{97}\text{Zr}$

### 6.2.2 Measurement of $^{94}\text{Zr}(n,\gamma)^{95}\text{Zr}$ reaction cross-section at $E_n=2.45$ MeV, Purnima

#### Neutron Generator (PNG), B.A.R.C, Mumbai

Purnima Neutron Generator (PNG) [24, 25] is 300 KV DC electrostatic accelerator (based on Cockcroft and Walten type multiplier) (Fig. 6. 2) in which  $\text{D}^+$  ion beam is accelerated at 100 kV and bombarded on deuterium target. It produces monoenergetic neutrons of energy 2.45 MeV based on the  $\text{D}(\text{D}, \text{n})^3\text{He}$  fusion reaction.  $\text{D}^+$  beam current is extracted from RF ion source and focused with einzel lens. A beam is accelerated up to 300 keV on titanium-tritiated target (TiT) with copper backing plate. The beam power dissipated in the TiT is removed with chilled water circulating around target. The neutron production is regulated by acceleration voltage and RF ion source parameters. The operating parameters of the neutron generator for the experiment are 115  $\mu\text{A}$   $\text{D}^+$  ion beam current and vacuum inside the system is maintained at pressure of  $3 \times 10^{-6}$  mbar. The operation of the PNG is controlled by PLC based control unit from outside the neutron generator hall.

Natural zirconium metal foil of known amount (0.0952 gm) with thickness of 1 mm and indium metal foil (flux monitor) of amount 0.057 gm with same thickness as Zr metal foil were wrapped separately with 0.025 mm thick super pure aluminum foil. These samples were placed at the neutron source at zero degree with respect to the incident beam direction and irradiated for the period of 2 hours and 30 minutes. After sufficient cooling, high resolution  $\gamma$ -ray spectrometry of these activated samples was performed using energy and efficiency calibrated HPGe detector as mentioned in the section 6.2.1. The HPGe detector assembly was kept in lead shielding of 5 cm thick. This lead shielding was having a 1 cm thick layer of stainless steel to minimize the Compton scattering and to absorb the x-rays from the lead. The  $\gamma$ -ray spectra were analyzed using the PHAST peak fitting program.



**Fig. 6.2 Photograph of Purnima Neutron Generator (300 KV DC electrostatic accelerator) at Bhabha Atomic Research Centre (B.A.R.C.), Mumbai**

### 6.2.3 Measurement of $^{90}\text{Zr}(n,p)^{90}\text{Y}^m$ reaction cross-section at average $E_n = 9.85 \pm 0.38$ MeV, T.I.F.R-B.A.R.C Pelletron Facility, Mumbai

The experiment was carried out using 14 UD BARC-TIFR Pelletron facilities at Mumbai, India. The neutron beam was produced from the  $^7\text{Li}(p,n)^7\text{Be}$  reaction [26] at six meter height main line above the analyzing magnet to utilize the maximum proton current from the accelerator. The lithium foil was made of natural lithium of thickness  $3.7 \text{ mg/cm}^2$  and wrapped with tantalum foil. The front tantalum foil facing the proton beam was of thickness  $3.9 \text{ mg/cm}^2$ , in which degradation of proton energy was only 30 keV. On the other hand, the back tantalum foil was thick enough to stop the proton beam. A known amount (0.1694 gm) of natural Zr metal foil, 1 mm thick natural indium metal foil and  $^{232}\text{Th}$  metal foil of area  $1 \text{ cm}^2$  with thickness of 0.025 mm were wrapped separately with 0.025 mm thick super pure aluminum foil to prevent contamination. The Zr-In-Th stack was mounted at zero degree with respect beam direction at a distance of 2.1 cm from the location of the Ta-Li-Ta stack. A schematic diagram for this experimental setup is shown in Fig. 6.3. These samples were irradiated for 4 hours with the neutron spectra generated from  $^7\text{Li}(p, n)^7\text{Be}$  reaction using proton beam of 12 MeV. The proton current during the irradiation was 400 nA. The average neutron energy for 12 MeV proton beam was calculated as  $9.85 \pm 0.38$  MeV. The detailed calculation of average neutron energy has already been explained in chapter 4. The irradiated samples Zr and In along with Al wrapper were cooled for two hours, mounted on two different perspex plates and taken for  $\gamma$ -ray spectrometry as mentioned in section 6.2.1. The  $\gamma$ -ray spectra were analyzed using PHAST peak fitting program.



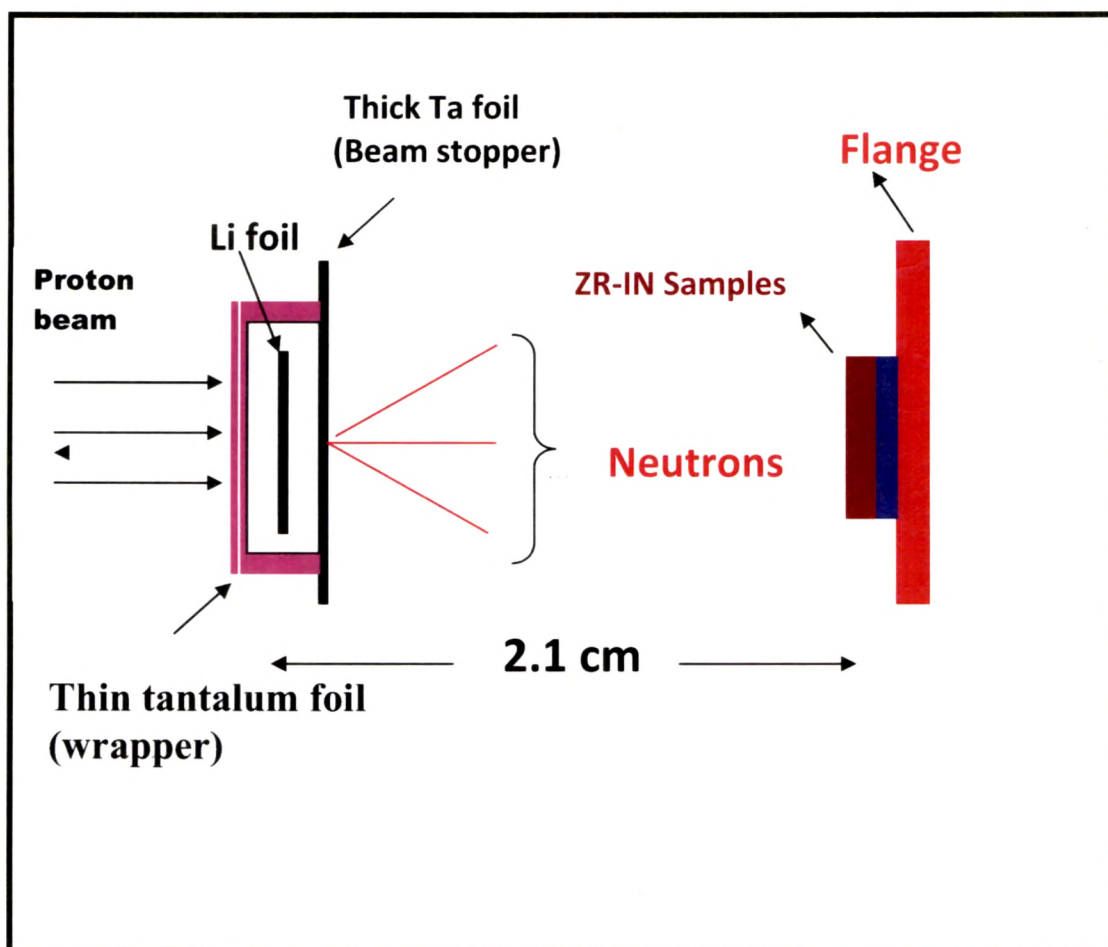


Fig. 6.3 Schematic diagram showing the arrangement used for neutron irradiation

## 6.3 Calculations

### 6.3.1 Calculations of neutron flux

For the thermal neutron activation cross-section measurements, the neutron flux was calculated using Au monitor. The photo-peak activity of 411.80 keV  $\gamma$ -lines of  $^{198}\text{Au}$  from  $^{197}\text{Au}(n, \gamma)^{198}\text{Au}$  reaction was used for flux determination. At higher neutron energy of 2.45 MeV and  $9.85 \pm 0.38$  MeV, the reaction  $^{115}\text{In}(n, n')^{115}\text{In}^m$  was used as a flux monitor. The photo-peak activity of 336.24 keV  $\gamma$ -lines of  $^{115}\text{In}^m$  from  $^{115}\text{In}(n, n')^{115}\text{In}^m$  was used for neutron flux determination. The observed photo-peak activity of gamma-lines was related to neutron flux ( $\phi$ ) with the relation as given below,

$$A_{obs} \left( \frac{CL}{LT} \right) = N \sigma \phi \alpha \varepsilon (1 - e^{(-\lambda t)} e^{(-\lambda T)} (1 - e^{(-\lambda CL)}) / \lambda \quad (1)$$

where,

$N$  = number of target atoms

$\sigma$  = monitor reaction cross-section

$\alpha$  = branching intensity  $\gamma$ -lines

$\varepsilon$  = branching detection efficiency

$t$  = irradiation time

$T$  = cooling time

$CL$  = clock time

$LT$  = counting time

The observed photo-peak activities of 411.80 KeV of  $^{198}\text{Au}$  and 336.24 KeV of  $^{115}\text{In}^m$  lines were obtained using PHAST peak fitting program. By taking the standard cross-sections ( $\sigma$ ) values [27], neutron flux was calculated separately for three irradiations. The nuclear

spectroscopic data such as half-life,  $\gamma$ -ray energy, branching intensity were taken from NuDat (BNL, U.S.A) [28] and are given in Table 6.1.

**Table 6.1 Nuclear Spectroscopic Data**

Nuclide	Half life	$\gamma$ -ray energy (keV)	$\gamma$ -ray abundance (%)
$^{198}\text{Au}$	2.272 d	411.80	95.62
$^{115}\text{In}^{\text{m}}$	4.486 h	336.24	45.80
$^{95}\text{Zr}$	64.03 d	724.19	44.27
		756.72	54.38
$^{97}\text{Zr}$	16.74 h	743.36	93.69
$^{90}\text{Y}^{\text{m}}$	3.19 h	202.53	97.30
		479.51	90.74

Using Eq. (1), we have calculated neutron flux as  $1.105 \times 10^8 \text{ n cm}^{-2} \text{ sec}^{-1}$  and  $2.1 \times 10^5 \text{ n cm}^{-2} \text{ sec}^{-1}$  for the thermal neutron energies (0.0253 eV) and 2.45 MeV respectively. The neutron flux for average neutron energy of  $9.85 \pm 0.38 \text{ MeV}$  was calculated as be  $(1.3 \pm 0.05) \times 10^7 \text{ n cm}^{-2} \text{ s}^{-1}$ . The detailed calculation of neutron flux has already been given in chapter 4.

### 6.3.2 Calculation of neutron cross-sections

The nuclear data used for the calculation of  $^{94}\text{Zr}(n,\gamma)^{95}\text{Zr}$ ,  $^{96}\text{Zr}(n,\gamma)^{97}\text{Zr}$  and  $^{90}\text{Zr}(n,p)^{90}\text{Y}^m$  reaction cross-sections were taken from NuDat (BNL, U. S. A). From the observed photo-peak activity of 756.72 keV  $\gamma$ -line of  $^{95}\text{Zr}$ , which has a half-life of 64.02 days,  $^{94}\text{Zr}(n,\gamma)^{95}\text{Zr}$  was calculated using decay-growth equation at thermal neutron energy and at  $E_n = 2.45 \text{ MeV}$ . Similarly, the observed photo-peak activity of 743.36 keV  $\gamma$ -line of  $^{97}\text{Zr}$  was used to calculate  $^{96}\text{Zr}(n,\gamma)^{97}\text{Zr}$  at thermal neutron energy. For the calculation of  $^{90}\text{Zr}(n,p)^{90}\text{Y}^m$  reaction cross-section, the observed photo-peak activities of 202.53 keV and 479.51 keV  $\gamma$ -lines of  $^{90}\text{Y}^m$  having half-life of 3.19 hours, was used. The observed photo-peak activities of corresponding  $\gamma$ -lines of  $^{95}\text{Zr}$ ,  $^{97}\text{Zr}$  and  $^{90}\text{Y}^m$  were obtained by using PHAST peak fitting program. Eq. (1) was used for the calculation of neutron reaction cross-section ( $\sigma$ ), according to which, it is given as follows

$$\sigma = \frac{A_{obs} \left( \frac{CL}{LT} \right) \lambda}{N_{pax} (1 - e(-\lambda t)) e(-\lambda T) (1 - e(\lambda CL))} \quad (1)$$

The  $^{94}\text{Zr}(n,\gamma)^{95}\text{Zr}$  and  $^{90}\text{Zr}(n,p)^{90}\text{Y}^m$  reaction cross-sections determined in the present work at neutron energies of 2.45 and  $9.85 \pm 0.38 \text{ MeV}$  are given in the Table 6.2. The  $^{94}\text{Zr}(n,\gamma)^{95}\text{Zr}$  and  $^{96}\text{Zr}(n,\gamma)^{97}\text{Zr}$  reaction cross-section determined in the present work at thermal neutron energy are also given in Table 6.2.

The uncertainties shown in the measured neutron reaction cross-sections are the precision values from two measurements, based on two different  $\gamma$ -lines. The overall uncertainty represents contribution from both random and systematic errors. The random error in the observed activity is primarily due to the counting statistics and is estimated to be 10-15%, which can be determined by accumulating the data for an optimum time period that depends on the half-life of the nuclides of interest. On the other hand, the systematic error is due to uncertainties in the irradiation time ( $\sim 2\%$ ), in the detection efficiency calibration ( $\sim 3\%$ ), in the half-life of the

reaction products and in the  $\gamma$ -ray abundances ( $\sim 2\%$ ). The overall systematic error is about 4 %.

The overall uncertainty for the cross-section is obtained about 11-16 %.

**Table 6.2 Experimentally measured neutron cross-sections ( $\sigma$ ) of Zr isotopes**

Energy	Reaction	$\sigma$ (mb)	IAEA- EXFOR (mb)	JENDL 4.0 (mb)	ENDF/B- VII (mb)	TENDL 2010 (mb)
Thermal	$^{94}\text{Zr}(n,\gamma)^{95}\text{Zr}$	$51.25 \pm 7.68$	47 - 75	50.69	49.88	49.89
Thermal	$^{96}\text{Zr}(n,\gamma)^{97}\text{Zr}$	$24.30 \pm 3.88$	20 - 100	20.32	22.85	22.85
2.45 MeV	$^{94}\text{Zr}(n,\gamma)^{95}\text{Zr}$	$5.41 \pm 0.59$	-----	2.67	7.65	6.52
$9.85 \pm 0.38$ MeV	$^{90}\text{Zr}(n,p)^{90}\text{Y}^{\text{m}}$	$3.1 \pm 0.45$	2.5- 3.4 <sup>a</sup>	-----	----- -	4.75

<sup>a</sup>Value quoted within the energy range of 9 – 10 MeV.

## 6.4 Result and Discussions

The  $^{94}\text{Zr}(n,\gamma)^{95}\text{Zr}$  and  $^{90}\text{Zr}(n,p)^{90}\text{Y}^{\text{m}}$  reaction cross-sections were measured at neutron energies of 2.45 MeV and  $9.85 \pm 0.38$  MeV respectively. The  $^{94}\text{Zr}(n,\gamma)^{95}\text{Zr}$  and  $^{96}\text{Zr}(n,\gamma)^{97}\text{Zr}$  reaction cross-sections were re-measured at thermal neutron energy. The measured cross-sections data from the present work are given in Table 6.2 along with the literature data available in IAEA-EXFOR database. The experimentally measured reaction cross-sections from the present work were compared with the evaluated nuclear data libraries from ENDF/B-VII, JENDL 4.0 and TENDL 2010. It is seen from Table 6.2 that the experimental data for  $^{94}\text{Zr}(n,\gamma)^{95}\text{Zr}$  and  $^{96}\text{Zr}(n,\gamma)^{97}\text{Zr}$  reactions at thermal neutron energy (0.0253 eV) from literature available in IAEA-EXFOR have a wide range from 47 to 75 mb and 20 to 100 mb respectively. The present cross-section data is well within this range of IAEA-EXFOR data at thermal neutron energy. It can also be seen from Table 6.2 that experimentally measured cross-sections values for the  $^{94}\text{Zr}(n,\gamma)^{95}\text{Zr}$  and  $^{96}\text{Zr}(n,\gamma)^{97}\text{Zr}$  reactions at thermal neutron energy are very close with the evaluated data from ENDF/B-VII JENDL 4.0 and TENDL 2010. This indicates that the present measurement of the neutron reaction cross-sections using activation technique and off-line  $\gamma$ -ray spectrometric technique is accurate. However, the experimentally measured  $^{94}\text{Zr}(n,\gamma)^{95}\text{Zr}$  reaction cross-section at neutron energy of 2.45 MeV is quite higher than JENDL 4.0 and lower than ENDF/B-VII, while it is in fair agreement with TENDL 2010. Further, the experimentally measured  $^{90}\text{Zr}(n,p)^{90}\text{Y}^{\text{m}}$  reaction cross-section at average neutron energy of  $9.85 \pm 0.38$  is in good agreement within the range of 9 MeV to 10 MeV data from IAEA-EXFOR database.

The experimentally measured  $^{94}\text{Zr}(n,\gamma)^{95}\text{Zr}$  and  $^{90}\text{Zr}(n,p)^{90}\text{Y}^{\text{m}}$  reaction cross-sections were plotted along with the experimental data available in IAEA-EXFOR database and with TENDL 2010 in the Figs. 6.4 and 6.5 respectively. It can be seen from Fig. 6.4 that the  $^{94}\text{Zr}(n,\gamma)^{95}\text{Zr}$  reaction cross-section decreases sharply with increase of neutron energy. This is due to opening of other reaction channels such as  $(n, \alpha)$ ,  $(n, 2n)$  etc., beyond 3 MeV region of neutron energy. It can also be seen from Fig. 6.5 that the experimental measured  $^{90}\text{Zr}(n,p)^{90}\text{Y}^{\text{m}}$  reaction cross-section at average neutron energy of  $9.85 \pm 0.38$  from the present work is consistent with the literature data available in IAEA-EXFOR database, which is shown by filled square.

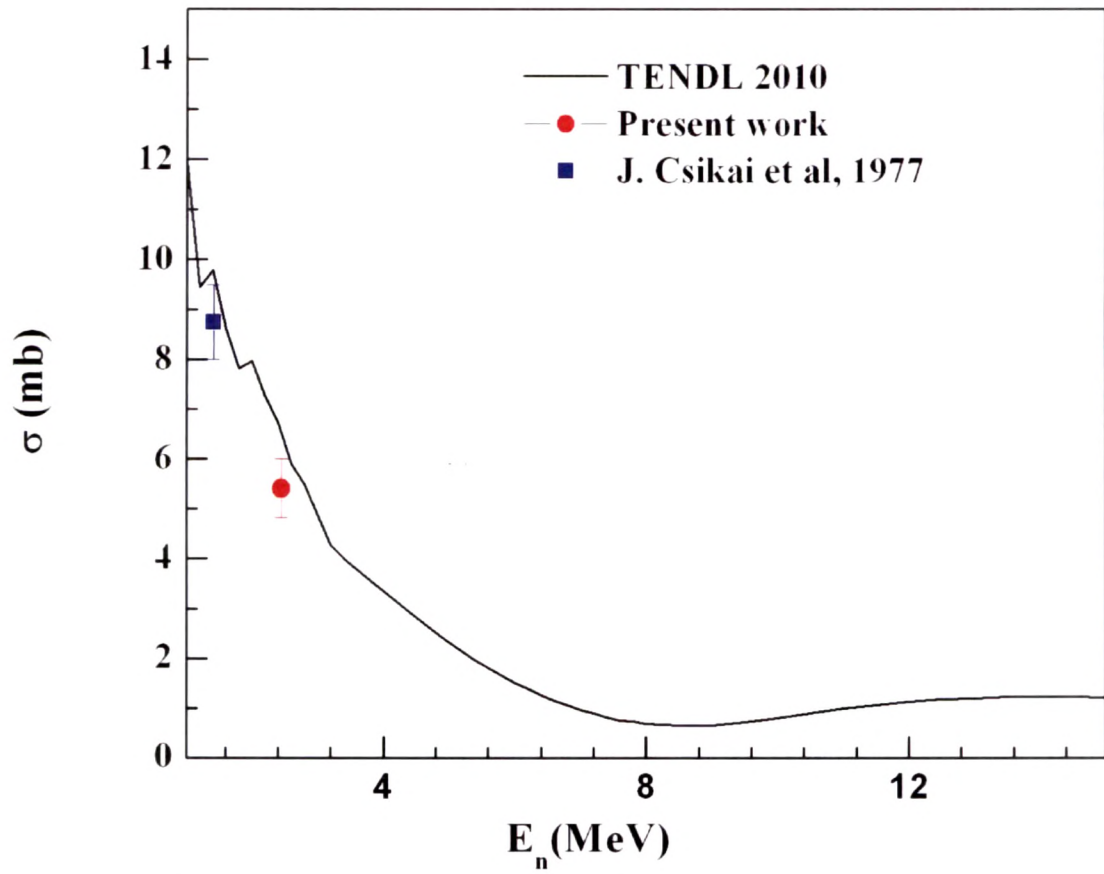


Fig. 6.4 Plot of experimental and evaluated  $^{94}\text{Zr}(n,\gamma)^{95}\text{Zr}$  reaction cross-section as a function of neutron energy 1 MeV to 15 MeV. Experimental values from the present work and from ref.29 are in different symbols and colors, whereas the evaluated values from TENDL 2010 are in black solid line.

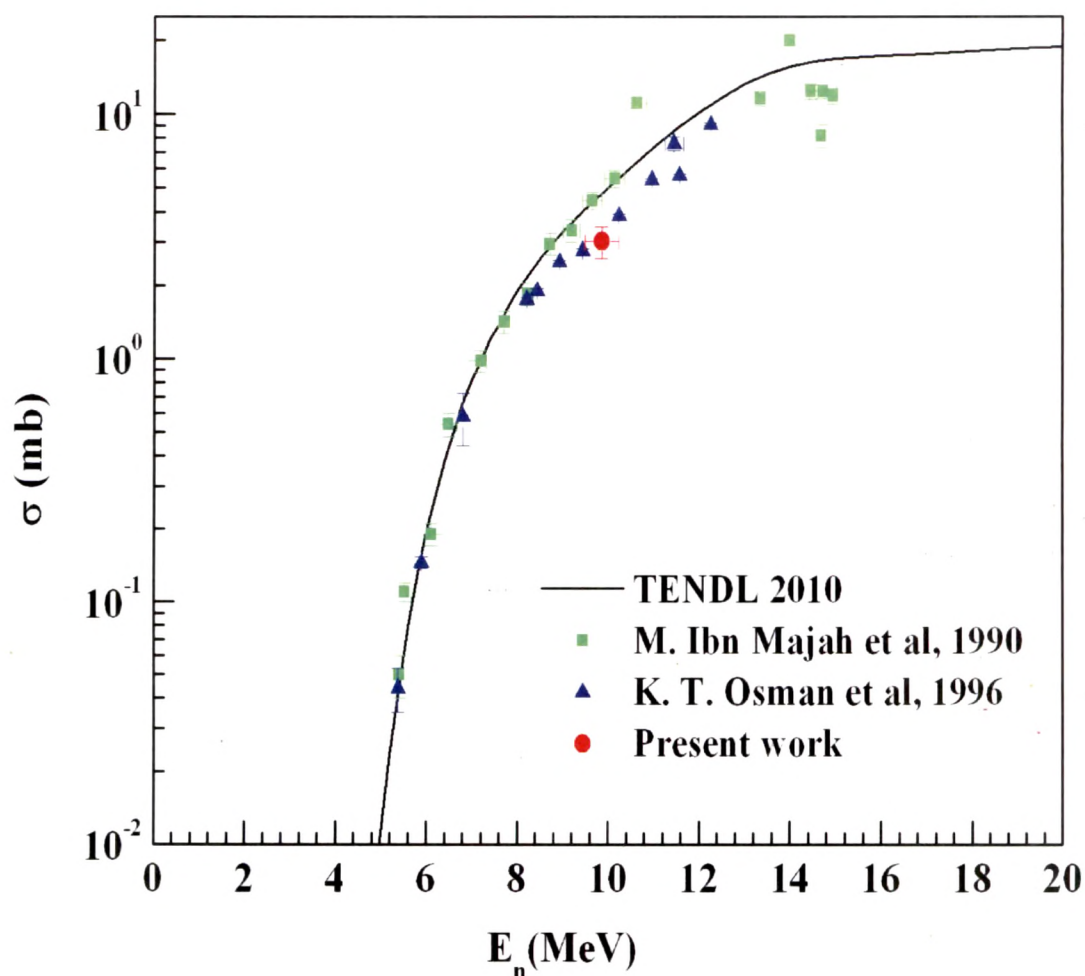


Fig. 6.5 Plot of experimental and evaluated  $^{90}\text{Zr}(n, p)^{90}\text{Y}^m$  reaction cross-section as a function of neutron energy 2 MeV to 20 MeV. Experimental values from the present work and from ref. (30, 31) are in different symbols and colors, whereas the evaluated values from TENDL 2010 are in black solid line



## 6.5 Summary and Conclusions

The  $^{94}\text{Zr}(n,\gamma)^{95}\text{Zr}$  and  $^{90}\text{Zr}(n,p)^{90}\text{Y}^{\text{m}}$  reaction cross-sections have been measured at neutron energies ( $E_n$ ) of 2.45 MeV and  $9.85 \pm 0.38$  MeV (average) using activation and off-line  $\gamma$ -ray spectrometric technique. For the measurement of  $^{94}\text{Zr}(n,\gamma)^{95}\text{Zr}$  reaction cross-section at  $E_n$  of 2.45, Purnima Neutron Generator (PNG) facility at B.A.R.C, Mumbai has been utilized. The  $^{90}\text{Zr}(n,p)^{90}\text{Y}^{\text{m}}$  reaction cross-section at average  $E_n$  of  $9.85 \pm 0.38$  MeV has been measured using BARC-TIFR Pelletron facility, Mumbai. The average neutrons of energy  $9.85 \pm 0.38$  MeV have been produced using  $^7\text{Li}(p,n)^7\text{Be}^*$  reaction at the six meter height main line above the analyzing magnet to utilize the maximum proton current from the accelerator. The “thermal neutron” activation cross-sections of  $^{94}\text{Zr}(n,\gamma)^{95}\text{Zr}$  and  $^{96}\text{Zr}(n,\gamma)^{97}\text{Zr}$  reactions were measured using the same technique in the thermal column of swimming pool type APSARA reactor, B. A. R. C, Mumbai, India. The experimentally measured neutron cross-sections data were compared with latest available evaluated nuclear data libraries from ENDF/B-VII, JENDL 4.0 and TENDL 2010. The following conclusions have been drawn from this work.

- The  $^{94}\text{Zr}(n,\gamma)^{95}\text{Zr}$  reaction cross-sections is measured for the first time at neutron energy of 2.45 MeV using neutron activation and off-line  $\gamma$ -ray spectrometric technique.
- The  $^{94}\text{Zr}(n,\gamma)^{95}\text{Zr}$  reaction cross-section at neutron energy of 2.45 MeV is higher than JENDL 4.0 and lower than ENDF/B-VII, while it is in fair agreement with TENDL 2010.
- The  $^{94}\text{Zr}(n,\gamma)^{95}\text{Zr}$  and  $^{96}\text{Zr}(n,\gamma)^{97}\text{Zr}$  reaction cross-sections are re-measured at thermal neutron energy. The experimentally measured cross-sections for the  $^{94}\text{Zr}(n,\gamma)^{95}\text{Zr}$  and  $^{96}\text{Zr}(n,\gamma)^{97}\text{Zr}$  reactions at thermal neutron energy are found to be very close with the evaluated data from ENDF/B-VII, JENDL 4.0 and TENDL 2010.
- The measured  $^{90}\text{Zr}(n,p)^{90}\text{Y}^{\text{m}}$  reaction cross-sections at average neutron energy of  $9.85 \pm 0.38$  from the present work is found consistent with data available in IAEA-EXFOR database.
- The present measurements have added new data points to the existing database.

## References:

- [1]. C. Rubbia et al, Conceptual Design of a Fast Neutron Operated High Power Energy Amplifier, CERN/AT/95-44 (ET) 1995
- [2]. S. Ganesan, Pramana J. Phys., **68**, 257 (2007)
- [3]. R. A. Forrest, J. Kopecky and J. C. Sublet, J. Nucl. Sci. and Technol., **S2**:96-99, 2002.
- [4]. J. Blomgren, Nuclear data for single-event, Proc. of the workshop on Neutron Measurement, Evaluations and applications, 5-8 November, Budapest, Hungary, EUR Report 21110 EN, ISBN 92-894-6041-5, 2003
- [5]. S. M. Qaim, Some applications of neutrons in biology and medicine, Proc. of the workshop on Neutron Measurement, Evaluations and applications, 5-8 November, Budapest, Hungary, EUR Report 21110 EN, ISBN 92-894-6041-5, 2003
- [6]. B. Lalremruata, S. D. Dhole, S. Ganesan, V. N. Bhoraskar, Nucl. Phys. A, **821** (2009) 23-35
- [7]. R. A. Forrest, Fusion Eng. Design, **81** (2006) 2143
- [8]. G. Aliberti, G. Palmiotti, M. Salvatores, T. Kim, T. Taiwo, M. Anitescu, I. Kodeli, E. Sartori, J. Bosq, J. Tomasi, Ann. Nucl. Energy, **33** (2006) 700
- [9]. V. Mclane, C. L. Dunford and P. F. Rose, "Neutron Cross-Sections," Vol. 2, Academic Press, San Diego (1988)
- [10]. R. C. Ward, I. C. Gomes and D. L. Smith, "A survey of selected neutron activation reactions with short-lived products of importance to fusion reactor technology," Report IAEA- INDC (USA) - **106**, Vienna (1994)
- [11]. IAEA-EXFOR Database, at <http://www-nds.iaea.org/exfor>
- [12]. R. L. Macklin, N. H. Lazar and W. S. Lyon, Phys. Rev., **107**, 2, 504 (1957)
- [13]. W. S. Lyon, Nucl. Sci. Eng., **8**, 378 (1960)
- [14]. D. J. Hughes and R. B. Schwartz, "Neutron Cross Sections," Report BNL – 325, second edition, Brookhaven National Laboratory (1958)
- [15]. C. M. Lederer, J. M. Hollander and I. P. Perlman, "Table of Isotopes," 6th ed., John Wiley and Sons, New York (1968)
- [16]. M. D. Ricabarra, R. Turjanski and G. H. Ricabarra, Can. J. Phys., **48**, 2362 (1970)
- [17]. R. H. Fulmer, D. P. Stricos and T. F. Ruane, Nucl. Sci. Eng., **46**, 314 (1971)
- [18]. D. C. Santry and R. D. Werner, Can. J. Phys., **51** 2441 (1973)

- [19]. S. F. Mughabghab and D. I. Garber, Neutron Cross Sections, Vol. I, Resonances, U. S. Dept. of Commerce, Virginia (1973)
- [20]. M. B. Chadwick et al., Nucl. Data Sheets, **107**, 2931 (2006)
- [21]. K. Shibata et al., J. Nucl. Sci. Technol., **48**, 1, (2011)
- [22]. A. J. Koning and D. Rochman, TENDL – 2010: Talys Evaluated Nuclear Data Library,” [www.talys.eu/tendl2010/](http://www.talys.eu/tendl2010/)
- [23]. P. K. Mukhopadhyaya, Personal Communication (2001)
- [24]. T. Patel, S. Bisnoi and A. Sinha, 2.45 MeV/14 MeV Neutron Generator Facility, Proc. 18<sup>th</sup> NSRP-2009, M. L. S University, Udaipur, Rajasthan, India
- [25]. S. Bisnoi, T. Patel, R. K. Pual, P. S. Sarkar, P. S. Adhikari and A. Sinha, Proc. of the DAE symp. on Nucl. Phys. 56 (2011)
- [26]. S. G. Mashnik et al, <sup>7</sup>Li(p,n) Nuclear data Library for Incident Proton Energies to 150 MeV,” arXiv: nucl-th/0011066v117, Los Alamos National Laboratory (Nov.2000).
- [27]. The international Reactor Dosimetry File:IRDF-2002,” Nuclear Data Section, International Atomic Energy Agency; at <http://www-nndc.bnl.gov/undocsc/libraries/irdf/>
- [28]. NuDat (BNL, U.S. A), [www.nndc.bnl.gov/nudat2/](http://www.nndc.bnl.gov/nudat2/)
- [29]. J. Csikai and Z. Dezso, Average cross-sections for the Cf-252 neutron spectrum. (n, g), (n, p), (n, a) and (n, 2n) reactions,” All Union Conference on Neutron Physics, Kiev, 18-22 April, 3, 32 (1977)
- [30]. M. Ibn Majah and S. M. Qaim, Nucl. Sci. Eng., **104**, 271 (1990)
- [31]. K. T. Osman and F. I. Hubbani, Measurement and study of (n, p) reaction cross-sections for Cr, Ti, Ni, Co, Zr and Mo isotopes using 14.7 neutrons, R, INDC(SUD)- 001, 1996